Mon. Not. R. Astron. Soc. **372,** 163–173 (2006) doi:10.1111/j.1365-2966.2006.10811.x

An activity catalogue of southern stars

J. S. Jenkins,[1⋆] H. R. A. Jones,[1] C. G. Tinney,[2] R. P. Butler,[3] C. McCarthy,[4] G. W. Marcy,[4,5] D. J. Pinfield,[1] B. D. Carter[6] and A. J. Penny[7,8,9]

[1]*Centre for Astrophysics Research, University of Hertfordshire, College Lane, Hatfield, Hertfordshire AL10 9AB*
[2]*Anglo-Australian Observatory, PO Box 296, Epping, NSW 1710, Australia*
[3]*Carnegie Institute of Washington, Department of Terrestrial Magnetism, 5241 Broad Branch Road NW, Washington, DC 20015-1305, USA*
[4]*Department of Physics and Astronomy, San Francisco State University, San Francisco, CA 94132, USA*
[5]*Department of Astronomy, University of California, Berkeley, CA 94720, USA*
[6]*Faculty of Sciences, University of Southern Queensland, Toowoomba, 4350, Australia*
[7]*Rutherford Appleton Laboratory, Chilton, Didcot, Oxon OX11 0QX*
[8]*SETI Institute, 515 North Whisman Road, Mountian View, CA 94043, USA*
[9]*Harvard-Smithsonian Center for Astrophysics, 60 Garden St, MA 02138, USA*

Accepted 2006 July 14. Received 2006 July 14; in original form 2006 April 28

ABSTRACT

We have acquired high-resolution echelle spectra of 225 F6-M5 type stars in the Southern hemisphere. The stars are targets or candidates to be targets for the Anglo-Australian Planet Search. Ca II H& K line cores were used to derive activity indices for all of these objects. The indices were converted to the Mt. Wilson system of measurements and $\log R'_{\rm HK}$ values determined. A number of these stars had no previously derived activity indices. In addition, we have also included the stars from Tinney et al. using our Mt. Wilson calibration. The radial-velocity instability (also known as *jitter*) level was determined for all 21 planet-host stars in our data set. We find the jitter to be at a level considerably below the radial-velocity signatures in all but one of these systems. 19 stars from our sample were found to be active ($\log R'_{\rm HK} > -4.5$) and thus have high levels of jitter. Radial-velocity analysis for planetary companions to these stars should proceed with caution.

Key words: stars: activity – stars: low-mass, brown dwarfs – planetary systems – ultraviolet: stars.

1 INTRODUCTION

The Anglo-Australian Planet Search (AAPS) has been monitoring the radial velocities of over 200 main-sequence stars since 1998 January (e.g. Tinney et al. 2001). Radial-velocity searches are the cornerstones of current planet detections, giving rise to the bulk of the 171 extrasolar planets (Butler et al. 2006). However, dynamical activity in the stellar chromosphere (e.g. Queloz et al. 2001; Henry, Donahue & Baliunas 2002; Paulson, Cochran & Hatzes 2004) can mimic the radial-velocity signature of a planet. Indeed, it can be the primary source of uncertainty in attributing radial-velocity periodicities to a planetary companion, making the measurement of this activity in each planet search target star critical.

The level of activity associated with a target is most commonly determined by measuring the strength of the calcium H& K lines in stellar spectra. The Mt. Wilson (MW) HK Project (Duncan et al. 1991) has been utilizing this technique since the mid-1960s for over 100 stars; currently the project monitors over 400 dwarfs and giants. They have defined a $\log R'_{\rm HK}$ index, which various studies have shown to be a useful indicator of the level of radial-velocity instability (jitter) in F–K type dwarfs (e.g. Saar & Donahue 1997; Santos et al. 2002; Wright 2005). The Vienna-Kitt Peak National Observatory (KPNO) Ca II H& K survey (Strassmeier et al. 2000) has similar aims. Both these studies target Northern hemisphere stars. There are no such studies conducted in the Southern hemisphere that provide the continuous monitoring of activity that these projects in the north provide. Until recently (2006), there was only one large-scale activity analysis of solar-type stars in the Southern hemisphere and this was provided by Henry et al. (1996) at the Cerro Tololo Inter-American Observatory (CTIO). Gray et al. (2006) have recently published the results of a spectroscopic survey conducted on stars earlier than M0 out to 40 pc at the CTIO and the Stewart Observatory. These projects do not provide the long-term monitoring aspect of the MW Project, yet they provide us with a useful testbed to the conclusions drawn in the north, whilst also providing an independent sample for statistical analysis.

When the AAPS list was drawn up, the vast majority of targeted stars were not on the activity list compiled by Henry et al. (1996). Henry et al. acknowledge that their primary sample of 650 stars south of -25° only comprise around 50 per cent of the total number of solar-type stars in this region of the southern sky down to $V \sim 9$.

⋆E-mail: jsj@star.herts.ac.uk

© 2006 The Authors. Journal compilation © 2006 RAS

Hence, to measure the chromospheric Ca II H& K core emission for all AAPS targets not in the Henry et al. catalogue, we have taken spectra of 225 stars from the AAPS, a number of which had no previously derived activity indices. Also, the majority of these objects are already being monitored by the AAPS for the presence of planetary companions; however some are being scrutinized as potential target candidates for an expansion of the target list.

2 OBSERVATIONS AND REDUCTION

Six nights of observations were taken over a period of 4 yr and are listed in Tables 1 and 2. The observations were made using the University College London Echelle Spectrograph mounted on the 3.9-m Anglo-Australian Telescope (AAT), and followed the observing procedures described by Tinney et al. (2002). We used the EEV2 2048 × 4096 13.5-μm pixel detector, with a Ca II HK quantum efficiency (QE) of ∼65 per cent, for observations made on the nights of 2001 August 04, 2002 July 20, 2003 July 21 and 2005 June 16. The CCD was spatially binned by two to give effective slit lengths of 11, 14, 23.5 and 17.5 pixels. The dispersion at the Ca II H& K lines is 0.02 Å pixel^{-1}, giving resolutions of 3.5, 4, 6 and 4 pixels or 0.07, 0.08, 0.12 and 0.08 Å. The remaining nights of observations were conducted on 2004 August 23 and 24 using the Massachusetts Institute of Technology (MIT) and Lincoln Labs (MITTL3) 2048 × 4096 chip. The chip has relatively low QE (∼18 per cent) around the H& K line region; however as these are bright sources this presented no problems. The CCD setup was similar to the EEV2 chip giving effective slit lengths of 23.5 pixels. The dispersion was again similar to that of the EEV2 runs (0.02 Å pixel^{-1}) giving a resolution of 4.5 pixels or 0.09 Å.

225 F6-M5 dwarfs and subgiants were observed in seeing ranging from 0.7 to 1.4 arcsec through slits of sizes 1.0 × 3.5, 1.0 × 4.0 and 1.0 × 6.0 arcsec. We have also included the observations in Tinney et al. (2002) to complete this catalogue. Exposure times ranged from 30 to 900 s for the faintest objects. This provided signal-to-noise ratios per 0.02 Å wavelength pixel of between 10 and 80. The target stars were taken from the AAPS target list and were supplemented by calibration stars taken from the MW HK Project (Duncan et al. 1991). These are used to calibrate on to the MW system of measurements. All calibration stars are listed in Table 1, along with their visual magnitudes, colours, spectral types and derived activity indices.

The reduction was accomplished using standard ECHOMOP protocols (Mills, Webb & Clayton 1996). Prior to the ECHOMOP procedure, the files were prepared by performing a bias or overscan subtraction and rotating them to ECHOMOP'S desired alignment. Each of the five orders (142–146) was then traced, clipped, flat-fielded, and the scattered light was removed. No sky subtraction was needed as the sky brightness around the Ca II H& K lines is negligible compared to the brightness of our sources. Wavelength calibration was performed using ThAr arc spectra acquired for this purpose. The data acquired using the MITTL3 chip were then flux calibrated, as were the data from Tinney et al. (2002), in order to correct the blaze and inter-order sensitivity. This was accomplished using a measurement of the standard μ Col (Turnshek et al. 1990). None of the other three nights was flux calibrated. All spectra were then scrunched to a linear scale with binwidths of 0.02 Å. All stars were then cross-correlated with an observation of HD 216435, and the barycentric velocity for this star was applied, leaving a series of zero-velocity spectra. Jones et al. (2002) have shown that HD 216435 has a radial-velocity variation of 20 m s^{-1} over a period of 1326 d (3.7 yr). This is negligible when compared with the barycentric correction. The spectra were then normalized to the continuum region between 3991 and 4011 Å, which represents the outer bandpass region (R) we used to acquire our desired activity index ($S_{\rm AAT}$).

To determine robust Ca II H& K activity indices, we employed four bandpasses centred around the calcium H& K line cores. The V and R bandpasses both have square profiles with widths of 20 Å and are centred on the continuum at 3901 and 4001 Å, respectively. The K and H bandpasses have triangular profiles with full width at half-maximums (FWHMs) of 1.09 Å and are centred on the cores themselves, at 3933.667 and 3968.470 Å, respectively. Fig. 1 (upper panel) shows the final spectrum after the reduction procedure for the star HD 190248. All four passbands are highlighted for reference. The H& K line cores are clearly evident. This star has a spectral type of G5IV-V. We find this star to be chromospherically quiet, with a final $\log R'_{\rm HK}$ of −5.03. The lower plot in Fig. 1 highlights

Table 1. S and $\log R'_{\rm HK}$ activity values for all stars used to calibrate on to the MW system of measurements. Column headings: HD number; Henry Draper catalogue identifiers. Johnson $B-V$, V and Spec type all taken from *Hipparcos*. $S_{\rm AAT}$ *after* calibration on to the MW system. $S_{\rm MW}$ is the MW index used to perform this calibration, taken from column 5 of table 1 and columns 4–7 of table 3 from Duncan et al. (1991). $\log R'_{\rm HK,MW}$ are derived from Duncan et al. (1991).

HD	$B-V$	V	Spec type	$S_{\rm AAT}$	$S_{\rm MW}$	$\log R'_{\rm HK,AAT}$	$\log R'_{\rm HK,MW}$
Calibrators							
HD 1835	0.659	6.39	G3V	0.330 ± 0.002, 0.326 ± 0.002, 0.371 ± 0.002	0.347	−4.47, −4.47, −4.40	−4.44
HD 3443AB	0.715	5.57	K1V	0.184 ± 0.001, 0.191 ± 0.001	0.186	−4.87, −4.90	−4.89
HD 3795	0.718	6.14	G3/G5V	0.150 ± 0.001, 0.157 ± 0.001, 0.160 ± 0.001	0.156	−5.02, −5.03, −5.07	−5.04
HD 9562	0.639	5.75	G2IV	0.145 ± 0.001, 0.146 ± 0.001	0.144	−5.09, −5.10	−5.11
HD 10700	0.727	3.49	G8V	0.169 ± 0.001, 0.176 ± 0.001, 0.179 ± 0.001	0.173	−4.92, −4.94, −4.97	−4.95
HD 11131	0.654	6.72	G0	0.307 ± 0.002, 0.325 ± 0.002, 0.348 ± 0.002	0.336	−4.43, −4.47, −4.51	−4.45
HD 16673	0.524	5.79	F6V	0.221 ± 0.001, 0.225 ± 0.001, 0.239 ± 0.002	0.215	−4.61, −4.65, −4.67	−4.69
HD 23249	0.915	3.52	K0IV	0.132 ± 0.001, 0.142 ± 0.001, 0.142 ± 0.001	0.137	−5.16, −5.16, −5.21	−5.18
HD 26965	0.820	4.43	K1V	0.178 ± 0.001, 0.192 ± 0.001	0.208	−4.92, −4.97	−4.87
HD 30495	0.632	5.49	G3V	0.282 ± 0.002, 0.317 ± 0.002	0.292	−4.47, −4.55	−4.52
HD 81809	0.642	5.38	G2V	0.170 ± 0.001	0.160	−4.93	−4.90
HD 115617	0.709	4.74	G5V	0.166 ± 0.001, 0.178 ± 0.001	0.161	−4.92, 4.98	−5.01
HD 152391	0.749	6.65	G8V	0.387 ± 0.003, 0.458 ± 0.003	0.392	−4.36, −4.45	−4.44
HD 158614	0.715	5.31	G8IV-V	0.167 ± 0.001, 0.175 ± 0.001	0.163	−4.94, −4.98	−5.00
HD 219834AC	0.787	5.20	G6/G8IV	0.169 ± 0.001	0.164	−4.99	−5.02

Note: the photon-counting errors are indicative only, a random error of $\gtrsim$3 per cent must be taken into account in all instances. This error was estimated from measurements of τ Ceti.

Table 2. $S_{\rm AAT}$ and $\log R'_{\rm HK,AAT}$ for stars on or under consideration for the AAPS. Column headings: HD number, Henry Draper catalogue identifiers [numbers with associated asterisks (*) highlight planet bearing stars]. Johnson $B-V$, V and Spec type all taken from the *Hipparcos* catalogue. $S_{\rm AAT}$: the AAT activity index *after* calibration on to the MW system of measurements. For objects with multiple measurements, we have included all the individual indices. $\log R'_{\rm HK,AAT}$: final activity values generated following the Noyes et al. (1984) methodology.

HD	$B-V$	V	Spec type	$S_{\rm AAT}$	$\log R'_{\rm HK,AAT}$
Measurements					
2001 August 04					
∗HD 142	0.519	5.70	G1IV	0.161 ± 0.001	−4.95
∗HD 2039	0.656	9.00	G2/G3IV/V	0.180 ± 0.001	−4.89
HD 2587	0.748	8.46	G6V	0.152 ± 0.001	−5.07
HD 3823	0.564	5.89	G1V	0.160 ± 0.001	−4.97
HD 6735	0.567	7.01	F8V	0.173 ± 0.001	−4.89
HD 7199	0.849	8.06	K0IV/V	0.177 ± 0.001	−4.99
HD 7570	0.571	4.97	F8V	0.166 ± 0.001	−4.93
HD 9280	0.760	8.03	G5	0.148 ± 0.001	−5.09
HD 10180	0.629	7.33	G1V	0.165 ± 0.001	−4.96
HD 10647	0.551	5.52	F8V	0.213 ± 0.001	−4.70
HD 11112	0.637	7.13	G4V	0.158 ± 0.001	−5.00
∗HD 13445	0.812	6.12	K0V	0.302 ± 0.002	−4.64
HD 16417	0.653	5.78	G1V	0.148 ± 0.001	−5.08
∗HD 17051	0.561	5.40	G3IV	0.249 ± 0.002	−4.59
HD 18907	0.794	5.88	G8/K0V	0.147 ± 0.001	−5.11
HD 19632	0.678	7.29	G3/G5V	0.369 ± 0.002	−4.41
HD 20029	0.561	7.05	F7V	0.156 ± 0.001	−4.99
HD 20201	0.584	7.27	G0V	0.178 ± 0.001	−4.87
HD 20766	0.641	5.53	G2V	0.270 ± 0.002	−4.58
∗HD 20782	0.630	7.36	G3V	0.186 ± 0.001	−4.85
HD 20807	0.600	5.24	G1V	0.184 ± 0.001	−4.84
HD 22104	0.679	8.32	G3V	0.155 ± 0.001	−5.04
∗HD 23079	0.583	7.12	F8/G0V	0.163 ± 0.001	−4.95
HD 23127	0.690	8.58	G2V	0.162 ± 0.001	−5.00
HD 23484	0.870	6.99	K1V	0.508 ± 0.003	−4.43
HD 24112	0.560	7.24	F8V	0.155 ± 0.001	−5.00
HD 25587	0.543	7.40	F7V	0.164 ± 0.001	−4.93
HD 25874	0.667	6.74	G5IV-V	0.169 ± 0.001	−4.95
HD 26754	0.551	7.16	F7/F8V	0.159 ± 0.001	−4.97
∗HD 27442	1.078	4.44	K2IV	0.129 ± 0.001	−5.35
HD 28255	0.659	6.28	G4V	0.188 ± 0.001	−4.85
∗HD 30177	0.773	8.41	G8V	0.152 ± 0.001	−5.08
HD 30876	0.901	7.49	K2V	0.468 ± 0.003	−4.51
HD 31527	0.606	7.49	G2V	0.172 ± 0.001	−4.91
HD 36108	0.590	6.78	G3V	0.155 ± 0.001	−5.01
HD 38283	0.584	6.69	G0/G1V	0.161 ± 0.001	−4.97
HD 38382	0.580	6.34	F8/G0V	0.167 ± 0.001	−4.93
HD 38973	0.594	6.63	G2V	0.161 ± 0.001	−4.97
HD 40307	0.935	7.17	K3V	0.265 ± 0.002	−4.83
HD 202628	0.637	6.75	G5V	0.257 ± 0.002	−4.61
HD 204385	0.596	7.14	G0IV	0.166 ± 0.001	−4.94
HD 204961	1.521	8.66	M1V	0.985 ± 0.007	−5.10
HD 205390	0.879	7.14	K2V	0.426 ± 0.003	−4.53
HD 205536	0.755	7.07	G8V	0.164 ± 0.001	−5.01
HD 209268	0.564	6.88	F7V	0.156 ± 0.001	−4.99
HD 211317	0.650	7.26	G5III/IV	0.156 ± 0.001	−5.02
HD 212168	0.599	6.12	G3IV	0.161 ± 0.001	−4.97
∗HD 216437	0.660	6.04	G4IV-V	0.155 ± 0.001	−5.03
HD 217987	1.483	7.35	M2/M3V	1.081 ± 0.007	−5.01
HD 222237	0.989	7.09	K3V	0.296 ± 0.002	−4.84
HD 222335	0.802	7.18	K1V	0.238 ± 0.002	−4.77
2002 July 20					
GL551	1.807	11.01	M5Ve	10.686 ± 0.072	−4.28
GL729	1.510	10.37	M3.5Ve	6.188 ± 0.042	−4.29

Table 2 – *continued*

HD	$B-V$	V	Spec type	$S_{\rm AAT}$	$\log R'_{\rm HK,AAT}$
HD 1273	0.655	6.84	G2V	0.192 ± 0.001	−4.83
HD 1581	0.576	4.23	F9V	0.167 ± 0.001	−4.92
HD 2071	0.681	7.27	G8IV	0.184 ± 0.001	−4.88
HD 5133	0.936	7.15	K2V	0.464 ± 0.003	−4.56
HD 5562	0.808	7.17	G8IV	0.147 ± 0.001	−5.11
HD 7570	0.571	4.97	F8V	0.159 ± 0.001	−4.97
HD 7693	1.000	7.22	K2V	0.655 ± 0.004	−4.48
HD 8581	0.569	6.85	F8V	0.152 ± 0.001	−5.03
HD 9540	0.766	6.97	K0V	0.365 ± 0.002	−4.49
HD 12042	0.487	6.10	F8V	0.161 ± 0.001	−4.94
HD 13246	0.544	7.50	F8V	0.341 ± 0.002	−4.38
HD 17925	0.862	6.05	K1V	0.674 ± 0.004	−4.29
∗HD 22049	0.881	3.72	K2V	0.480 ± 0.003	−4.47
HD 23456	0.511	6.97	G1V	0.166 ± 0.001	−4.91
HD 27274	1.115	7.64	K5V	0.416 ± 0.003	−4.86
HD 30295	0.812	8.86	K0/K1V	0.142 ± 0.001	−5.13
HD 31827	0.770	8.26	G8IV	0.149 ± 0.001	−5.09
HD 33811	0.765	8.71	G8IV/V	0.164 ± 0.001	−5.01
HD 38110	0.696	8.18	G5	0.159 ± 0.001	−5.02
HD 38393	0.481	3.59	F7V	0.167 ± 0.001	−4.90
HD 40307	0.935	7.17	K3V	0.255 ± 0.002	−4.85
HD 84117	0.534	4.93	G0V	0.158 ± 0.001	−4.97
HD 85512	1.156	7.67	K5V	0.312 ± 0.002	−5.05
HD 85512	1.156	7.67	K5V	0.383 ± 0.002	−4.96
HD 85683	0.546	7.34	F8V	0.165 ± 0.001	−4.93
HD 85683	0.546	7.34	F8V	0.168 ± 0.001	−4.91
HD 85683	0.546	7.34	F8V	0.168 ± 0.001	−4.91
HD 97998	0.626	7.36	G5V	0.187 ± 0.001	−4.84
HD 101581	1.064	7.77	K5V	0.500 ± 0.003	−4.70
HD 101805	0.528	6.48	G1V	0.160 ± 0.001	−4.95
∗HD 102117	0.721	7.47	G6V	0.158 ± 0.001	−5.03
HD 103026	0.554	5.85	F8V	0.150 ± 0.001	−5.04
HD 103493B	0.646	6.70	G5V	0.194 ± 0.001	−4.82
HD 103975	0.527	6.76	G0V	0.162 ± 0.001	−4.94
HD 105328	0.613	6.72	G2V	0.161 ± 0.001	−4.97
HD 106453	0.711	7.47	K0/K1V	0.319 ± 0.002	−4.52
HD 106869	0.574	6.81	G1V	0.162 ± 0.001	−4.96
HD 110810	0.937	7.82	K3V	0.623 ± 0.004	−4.42
HD 112019	0.520	7.69	G0V	0.165 ± 0.001	−4.92
HD 113027	0.569	7.56	G2V	0.189 ± 0.001	−4.81
HD 114260	0.718	7.36	G6V	0.173 ± 0.001	−4.95
HD 114613	0.693	4.85	G3V	0.157 ± 0.001	−5.03
HD 114613	0.693	4.85	G3V	0.157 ± 0.001	−5.03
HD 115585	0.742	7.43	G6IV-V	0.152 ± 0.001	−5.07
HD 117105	0.583	7.20	G1V	0.167 ± 0.001	−4.93
HD 117939	0.669	7.29	G3V	0.181 ± 0.001	−4.89
HD 118475	0.618	6.97	G2/G3IV/V	0.166 ± 0.001	−4.95
HD 118972	0.855	6.92	K1V	0.503 ± 0.003	−4.42
HD 120780	0.891	7.37	K1V	0.264 ± 0.002	−4.79
HD 122862	0.581	6.02	G1V	0.157 ± 0.001	−4.99
HD 124584	0.590	7.29	G0/G1V	0.160 ± 0.001	−4.98
HD 125072	1.017	6.66	K3V	0.283 ± 0.002	−4.89
HD 125370	1.095	8.53	K0III	0.179 ± 0.001	−5.21
HD 128674	0.672	7.39	G5V	0.188 ± 0.001	−4.86
HD 129060	0.553	6.99	F7V	0.330 ± 0.002	−4.41
HD 134606	0.740	6.86	G5IV	0.157 ± 0.001	−5.04
∗HD 134987	0.691	6.47	G5V	0.155 ± 0.001	−5.04
HD 136352	0.639	5.65	G2V	0.176 ± 0.001	−4.90
HD 140785	0.660	7.38	G5V	0.154 ± 0.001	−5.04
HD 140901	0.715	6.01	G6IV	0.256 ± 0.002	−4.66
∗HD 142415	0.621	7.33	G1V	0.235 ± 0.002	−4.66
HD 143114	0.606	7.34	G3V	0.171 ± 0.001	−4.92
HD 144009	0.714	7.23	G8V	0.193 ± 0.001	−4.86
HD 144628	0.856	7.11	K3V	0.193 ± 0.001	−4.94
HD 145417	0.815	7.53	K0V	0.210 ± 0.001	−4.86

Table 2 – *continued*

HD	$B-V$	V	Spec type	$S_{\rm AAT}$	$\log R'_{\rm HK,AAT}$
HD 145809	0.617	6.68	G3V	0.154 ± 0.001	−5.02
HD 146481	0.642	7.09	G4V	0.160 ± 0.001	−4.99
HD 147723	0.625	5.40	G0IV	0.147 ± 0.001	−5.08
HD 147723	0.625	5.40	G0IV	0.159 ± 0.001	−4.99
HD 149612	0.616	7.01	G3V	0.179 ± 0.001	−4.87
HD 150474	0.780	7.16	G8V	0.148 ± 0.001	−5.10
HD 151337	0.901	7.38	K0V	0.147 ± 0.001	−5.13
HD 152311	0.685	5.86	G5IV	0.150 ± 0.001	−5.07
HD 153075	0.581	6.99	G0V	0.172 ± 0.001	−4.90
HD 154577	0.889	7.38	K0V	0.245 ± 0.002	−4.82
∗HD 154857	0.699	7.24	G5V	0.154 ± 0.001	−5.05
HD 155918	0.607	7.00	G2V	0.175 ± 0.001	−4.89
HD 155974	0.479	6.09	F6V	0.159 ± 0.001	−4.95
HD 156274	0.764	5.47	M0V	0.176 ± 0.001	−4.95
HD 157060	0.541	6.42	F8V	0.161 ± 0.001	−4.95
HD 159868	0.714	7.24	G5V	0.171 ± 0.001	−4.96
HD 162396	0.523	6.19	F8V	0.155 ± 0.001	−4.98
HD 162521	0.451	6.36	F8V	0.227 ± 0.001	−4.63
HD 163272	0.614	7.39	G2/G3V	0.163 ± 0.001	−4.96
HD 165269	0.611	7.29	G1V	0.170 ± 0.001	−4.92
HD 166553	0.599	7.27	G1/G2V	0.157 ± 0.001	−5.00
HD 168060	0.759	7.34	G5V	0.148 ± 0.001	−5.10
∗HD 169830	0.517	5.90	F8V	0.151 ± 0.001	−5.02
HD 171990	0.593	6.39	G2V	0.150 ± 0.001	−5.05
HD 179140	0.627	7.23	G2V	0.158 ± 0.001	−5.00
∗HD 179949	0.548	6.25	F8V	0.198 ± 0.001	−4.76
HD 183877	0.675	7.14	K0+..	0.183 ± 0.001	−4.88
HD 184509	0.557	6.74	G1V	0.174 ± 0.001	−4.88
HD 188641	0.626	7.34	G2V	0.159 ± 0.001	−5.00
HD 190248	0.751	3.55	G5IV-V	0.160 ± 0.001	−5.03
HD 191408	0.868	5.32	K2V	0.195 ± 0.001	−4.94
HD 191849	1.431	7.97	M0V	1.630 ± 0.011	−4.76
HD 192310	0.878	5.73	K3V	0.204 ± 0.001	−4.92
HD 192865	0.558	6.91	F8V	0.158 ± 0.001	−4.97
HD 193193	0.594	7.20	G2V	0.165 ± 0.001	−4.95
HD 196068	0.640	7.18	G5V	0.150 ± 0.001	−5.06
HD 196378	0.544	5.11	F8V	0.158 ± 0.001	−4.97
HD 196390	0.626	7.33	G3V	0.203 ± 0.001	−4.78
HD 196800	0.607	7.21	G1/G2V	0.162 ± 0.001	−4.97
HD 202457	0.689	6.60	G5V	0.161 ± 0.001	−5.00
HD 202560	1.397	6.69	M1/M2V	0.993 ± 0.007	−4.93
HD 203985	0.876	7.49	K0V	0.190 ± 0.001	−4.96
HD 204287	0.663	7.33	G3V	0.154 ± 0.001	−5.04
HD 206395	0.559	6.67	G0IV	0.162 ± 0.001	−4.95
HD 209100	1.056	4.69	K5V	0.450 ± 0.003	−4.74
HD 210272	0.663	7.22	G3V	0.152 ± 0.001	−5.05
HD 213042	1.080	7.65	K4V	0.325 ± 0.002	−4.92
∗HD 216435	0.621	6.03	G3IV	0.157 ± 0.001	−5.01
HD 216803	1.094	6.48	K4Vp	0.856 ± 0.006	−4.51
HD 219048	0.733	6.90	G5V	0.161 ± 0.001	−5.02
HD 221420	0.681	5.82	G2V	0.142 ± 0.001	−5.13
HD 222668	0.835	7.35	G8IV/V	0.150 ± 0.001	−5.09
HD 224619	0.741	7.47	G8V	0.184 ± 0.001	−4.91
HD 225213	1.462	8.56	M2V	0.383 ± 0.002	−5.43
2003 April 21st					
HD 4447	0.908	8.78	K0	0.157 ± 0.001	−5.10
HD 30876	0.901	7.49	K2V	0.393 ± 0.003	−4.59
HD 42902	0.623	8.92	G2/G3V	0.148 ± 0.001	−5.07
HD 44821	0.663	7.37	K0/1V	0.319 ± 0.002	−4.49
HD 44821	0.663	7.37	K0/1V	0.322 ± 0.002	−4.48
HD 45701	0.660	6.45	G3III/IV	0.157 ± 0.001	−5.02
HD 52447	0.605	8.38	G0V	0.148 ± 0.001	−5.06
HD 52447	0.605	8.38	G0V	0.149 ± 0.001	−5.06
HD 55693	0.660	7.17	G1V	0.164 ± 0.001	−4.98

© 2006 The Authors. Journal compilation © 2006 RAS, MNRAS **372,** 163–173

Table 2 – *continued*

HD	$B-V$	V	Spec type	$S_{\rm AAT}$	$\log R'_{\rm HK,AAT}$
HD 55720	0.705	7.50	G6V	0.166 ± 0.001	−4.98
HD 56560	0.737	7.33	G6IV/V	0.143 ± 0.001	−5.12
HD 59468	0.694	6.72	G5IV-V	0.162 ± 0.001	−5.00
HD 61686	0.693	8.54	G3V	0.136 ± 0.001	−5.18
HD 61686	0.693	8.54	G3V	0.144 ± 0.001	−5.12
HD 65907A	0.573	5.59	G2V	0.173 ± 0.001	−4.89
HD 67199	0.872	7.18	K1V	0.336 ± 0.002	−4.64
HD 67556	0.548	7.30	F8V	0.175 ± 0.001	−4.87
HD 69655	0.579	6.63	G1V	0.165 ± 0.001	−4.94
∗HD 70642	0.692	7.17	G8:III	0.167 ± 0.001	−4.97
∗HD 70642	0.692	7.17	G8:III	0.168 ± 0.001	−4.97
HD 70889	0.600	7.09	G0V	0.237 ± 0.002	−4.64
HD 72769	0.745	7.22	K1IV	0.147 ± 0.001	−5.10
HD 73121	0.578	6.44	G1V	0.169 ± 0.001	−4.92
HD 74868	0.567	6.56	G3IV	0.159 ± 0.001	−4.98
∗HD 76700	0.745	8.16	G8V	0.130 ± 0.001	−5.22
∗HD 76700	0.745	8.16	G8V	0.136 ± 0.001	−5.18
HD 78429	0.664	7.31	G5V	0.202 ± 0.001	−4.80
HD 80635	0.729	8.80	G3IV	0.135 ± 0.001	−5.18
HD 80635	0.729	8.80	G3IV	0.141 ± 0.001	−5.14
HD 80913	0.556	7.49	F6V	0.152 ± 0.001	−5.02
HD 88201	0.558	7.45	G0V	0.357 ± 0.002	−4.36
HD 90712	0.585	7.52	G2/G3V	0.388 ± 0.003	−4.32
HD 109200	0.836	7.13	K0V	0.189 ± 0.001	−4.94
2004 August 23 &24					
HD 7442	0.587	7.17	F8/G0V	0.151 ± 0.001	−5.04
HD 13578	0.620	7.50	G3IV	0.156 ± 0.001	−5.01
HD 16427	0.568	6.84	F8V	0.164 ± 0.001	−4.94
HD 17925	0.862	6.05	K1V	0.699 ± 0.005	−4.27
HD 21626	0.501	6.73	G0IV	0.147 ± 0.001	−5.05
∗HD 22049	0.881	3.72	K2V	0.563 ± 0.004	−4.39
HD 22924	0.552	6.94	F8/G0V	0.152 ± 0.001	−5.02
HD 23308	0.522	6.50	F8V	0.250 ± 0.002	−4.57
HD 28454	0.470	6.10	F8V	0.160 ± 0.001	−4.95
HD 31975	0.521	6.28	F8V	0.169 ± 0.001	−4.90
HD 32820	0.528	6.30	F8V	0.159 ± 0.001	−4.96
HD 33473	0.662	6.75	G3V	0.162 ± 0.001	−4.99
HD 34606	1.014	8.92	G5	0.168 ± 0.001	−5.14
HD 38393	0.481	3.59	F7V	0.158 ± 0.001	−4.96
∗HD 142415	0.621	7.33	G1V	0.260 ± 0.002	−4.59
HD 146481	0.642	7.09	G4V	0.181 ± 0.001	−4.88
HD 147722	0.625	5.40	G0	0.168 ± 0.001	−4.94
HD 147722	0.625	5.40	G0	0.181 ± 0.001	−4.87
HD 149612	0.616	7.01	G3V	0.205 ± 0.001	−4.76
HD 150474	0.780	7.16	G8V	0.166 ± 0.001	−5.00
HD 151337	0.901	7.38	K0V	0.158 ± 0.001	−5.09
HD 153075	0.581	6.99	G0V	0.195 ± 0.001	−4.79
HD 154577	0.889	7.38	K0V	0.252 ± 0.002	−4.81
∗HD 154857	0.699	7.24	G5V	0.173 ± 0.001	−4.94
HD 155974	0.479	6.09	F6V	0.162 ± 0.001	−4.93
HD 179140	0.627	7.23	G2V	0.175 ± 0.001	−4.90
∗HD 179949	0.548	6.25	F8V	0.209 ± 0.001	−4.72
HD 183877	0.675	7.14	K0	0.194 ± 0.001	−4.84
HD 188641	0.626	7.34	G2V	0.171 ± 0.001	−4.92
HD 192310	0.878	5.73	K3V	0.238 ± 0.002	−4.83
HD 192865	0.558	6.91	F8V	0.164 ± 0.001	−4.94
HD 193193	0.594	7.20	G2V	0.186 ± 0.001	−4.83
HD 196068	0.640	7.18	G5V	0.160 ± 0.001	−5.00
HD 196378	0.544	5.11	F8V	0.162 ± 0.001	−4.95
HD 196390	0.626	7.33	G3V	0.243 ± 0.002	−4.64
HD 196800	0.607	7.21	G1/G2V	0.160 ± 0.001	−4.98
HD 202560	1.397	6.69	M1/M2V	1.076 ± 0.007	−4.89
HD 202560	1.397	6.69	M1/M2V	1.111 ± 0.007	−4.88
HD 203985	0.876	7.49	K0V	0.188 ± 0.001	−4.96

Table 2 – *continued*

HD	$B-V$	V	Spec type	$S_{\rm AAT}$	$\log R'_{\rm HK,AAT}$
HD 203985	0.876	7.49	K0V	0.191 ± 0.001	−4.95
HD 204287	0.663	7.33	G3V	0.164 ± 0.001	−4.97
HD 207129	0.601	5.57	G2V	0.184 ± 0.001	−4.85
HD 212330	0.665	5.31	F9V	0.164 ± 0.001	−4.98
∗HD 216435	0.621	6.03	G3IV	0.164 ± 0.001	−4.96
HD 216803	1.094	6.48	K4Vp	1.084 ± 0.007	−4.41
HD 219048	0.733	6.90	G5V	0.162 ± 0.001	−5.01
HD 222668	0.835	7.35	G8IV/V	0.160 ± 0.001	−5.05
HD 224619	0.741	7.47	G8V	0.192 ± 0.001	−4.88
2005 June 16					
HD 56957	0.701	7.57	G3V	0.148 ± 0.001	−5.09
HD 63685	0.758	7.38	G5V	0.157 ± 0.001	−5.04
HD 67556	0.548	7.30	F8V	0.196 ± 0.001	−4.77
HD 69655	0.579	6.63	G1V	0.176 ± 0.001	−4.88
∗HD 70642	0.692	7.17	G8:III	0.175 ± 0.001	−4.93
HD 72769	0.745	7.22	K1IV	0.161 ± 0.001	−5.02
∗HD 73526	0.737	8.99	G6V	0.154 ± 0.001	−5.05
HD 74868	0.567	6.56	G3IV	0.165 ± 0.001	−4.93
∗HD 76700	0.745	8.16	G8V	0.160 ± 0.001	−5.02
HD 80913	0.556	7.49	F6V	0.166 ± 0.001	−4.93
HD 94340	0.645	7.02	G3/G5V	0.293 ± 0.002	−4.53
HD 95456	0.527	6.06	F8V	0.168 ± 0.001	−4.91
HD 142022	0.790	7.70	K0V	0.166 ± 0.001	−5.01

Note: the photon-counting errors are indicative only, a random error of $\gtrsim$3 per cent must be taken into account in all instances. This error was estimated from measurements of τ Ceti.

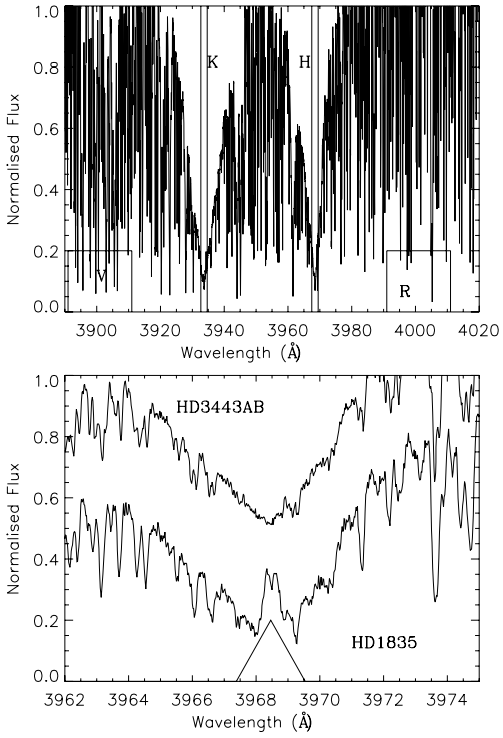

Figure 1. The calcium H& K emission features, obtained at the AAT, for the star HD 190248 (top panel). The R, V, H and K bandpasses are indicated for reference. The narrow features, other than H and K, are due to weak absorption lines not noise. The bottom panel shows the triangular bandpass used to integrate the flux for the Ca II H feature. The calibration stars shown are HD 3443AB (inactive: $\log R'_{\rm HK} = -4.89$) and HD 1835 (active: $\log R'_{\rm HK} = -4.45$). Both have been offset from zero for clarity.

the triangular bandpasses used to integrate the flux of the H line core. Two calibration stars are shown for reference, those are HD 3443AB (top panel) and HD 1835 (bottom panel), and both have been offset from zero for clarity. The stars are both main-sequence stars and have spectral types of K1V and G3V, respectively. The more active of the two (HD 1835) exhibits some marked emission at the central core, whereas the inactive star (HD 3443AB) has deep central minima. It is these characteristics that allow accurate activity indices to be generated.

3 ANALYSIS

3.1 *S* indices

Our spectra have been used to measure Ca II H& K emission ($S_{\rm MW}$) indices (Duncan et al. 1991). This index is a measure of the ratio between the integrated flux in two triangular bandpasses (with FWHMs of 1.09 Å) centred on the Ca II H (3968.470 Å) and K (3933.664 Å) lines, against the integrated flux in two square 20 Å continuum bandpasses at either side of the H& K features, centred at 3901 Å (V) and 4001 Å (R). The MW Project determines this index individually each night using a specialized multichannel photometer. $S_{\rm MW}$ is defined as

$$S_{\rm MW} = \alpha \frac{N_{\rm H} + N_{\rm K}}{N_{\rm R} + N_{\rm V}}, \quad (1)$$

where N_i is the number of counts in each bandpass (where i = H, K, V and R) and α is a constant that is determined each night by the observation of standards.

Using the same methodology used to determine equation (1), Tinney et al. (2002) have shown that the emission index for stars observed at the AAT ($S_{\rm AAT}$) is given by

$$S_{\rm AAT} = \frac{N_{\rm H,1} + N_{\rm H,2} + N_{\rm K,1} + N_{\rm K,2}}{2(N_{\rm R} + N_{\rm V})}. \quad (2)$$

© 2006 The Authors. Journal compilation © 2006 RAS, MNRAS **372,** 163–173

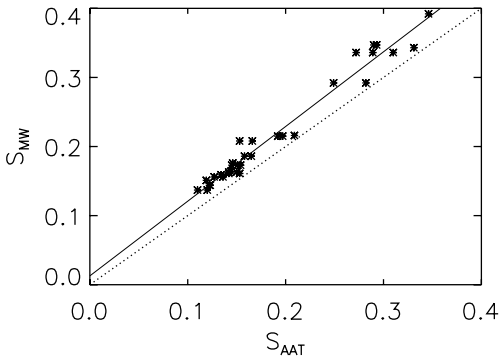

Figure 2. Calibration of the S_{AAT} index on to the S_{MW} system of measurements. The solid line represents a linear least-squares fit described by $S_{MW} = (1.081 S_{AAT}) + 0.013$, with a total rms scatter of 0.014. The dotted line shows a 1:1 relationship.

Here, the N_{HK} terms have two components. This is due to positioning of the echellogram, which causes both the H& K features to appear in two adjacent orders.

We used equation (2) to combine the integrated flux values from all bandpasses, giving us a set of S_{AAT} values we could use to calibrate on to the MW system of measurements. We have employed slightly different instrumental setups in our study and have observed our targets across a range of signal-to-noise ratios; therefore we have included individual measurements for multiple objects in our calibrations. We have also chosen the most stable calibrators possible from Duncan et al. (1991), allowing us a better estimation of the variability error in our final activity index. Columns 3 and 4 of Duncan et al. (1991) give the minimum and maximum S indices obtained at MW. Over the course of one observing season, the measured S index can vary on the level of ± 0.05, therefore selecting the most stable calibrators helps us reduce this uncertainty. Fig. 2 shows the least-squares fit used to calibrate on to S_{MW}. The calibration we employ (S_{AAT}) has a slope of 1.081 ± 0.001 and a zero-point offset of 0.013 ± 0.007. The rms scatter about the fit is 0.014. This level of scatter is lower than the scatter found by Tinney et al. (2002) who also calibrated against stars from the CTIO study. Henry et al. (1996) employed a different approach to both the MW Project and our AAT analysis. They centred 4 Å wide square bandpasses on the H& K line cores, compared to the 1.09-Å triangular bandpasses employed at MW. When the bandpasses here are widened, non-linear calibrations are needed to convert to the MW system of measurements. We suspect that this leads to increased systematic errors in H& K values. Indeed, when we include all objects in this study with CTIO indices in our calibration, we find a similar scatter to Tinney et al. (2002) of around 0.02.

Table 2 shows all derived S_{AAT} activity indices, after calibration on to the MW system of measurements, along with their 1σ photon-counting uncertainties. The table is split by epoch, and there are a few objects with more than one measurement. In the majority of cases, the photon-counting errors are an order of magnitude below that of the overall scatter from the calibration. In order to fully quantify all sources of error in the reduction procedure, such as scattered light removal, proper blaze removal, precise flux calibration, etc., we used the stable star HD 10700 (τ Ceti) as a proxy for the reduction errors. We have acquired three separate measurements of τ Ceti spanning a period of 3 yr, and due to the extremely small variation of $\sim$1 per cent (Baliunas et al. 1995) this represents a good indicator of the random errors in the reduction procedure. The standard deviation of the three measurements here is 3 per cent, which is slightly lower than that of the Keck and Lick errors from Wright et al. (2004). However, we only have three separate measurements, which likely give rise to a slightly lower estimation of the random errors. This 3 per cent error should also be taken into account when quantifying the significance of any of the activity indices in Table 2.

3.2 log R'_{HK} values

The S index provides an estimate of both the photospheric and chromospheric flux, and hence a combined Ca II emission feature. In order to obtain actual activity values, we have to concentrate on chromospheric flux, meaning photospheric effects have to be removed. This is accomplished by normalizing the chromospheric emission to the bolometric luminosity of the star, and is most commonly designated by the $\log R'_{HK}$ parameter. We have followed Noyes et al. (1984) to convert all main-sequence star values from S_{AAT} to $\log R'_{HK,AAT}$. We extrapolated the Noyes et al. conversion to include later spectral-types due to the lack of information on these stars. The Noyes et al. calibration is intended for stars in the colour range of $B - V \sim 0.44$–0.90, which means the final $\log R'_{HK}$ measurements of stars redder than 0.90 have a larger uncertainty than those in the calibration range. The derived values for the calibration stars are given in Table 1, along with the Duncan et al. $\log R'_{HK,MW}$ values. The values for all other objects are listed in Table 2. The *Hipparcos* $B - V$ and visual magnitudes are shown in both the tables for reference, and to highlight the photometric contribution to the S_{AAT} values.

In Fig. 3, we have plotted our $\log R'_{HK,AAT}$ values against the published values from Duncan et al. It can be seen from the gradient of the fit that there is good agreement with the MW data points. The gradient of the linear trend is 1.006 ± 0.001 with an offset of 0.023 ± 0.137. The rms of the fit is 0.041, highlighting just how tight our values are to the published MW data. By using all the measurements in the calibration, and not just the means, we allow the error to include any variability and systematic effects. The dotted line in the figure shows a direct 1:1 relationship, and it can be seen how close the $\log R'_{HK,MW}$ and $\log R'_{HK,AAT}$ are. We therefore employ no further calibration. Due to the inherently variable nature of stellar activity and errors in the reduction procedure, we believe the deduced rms is a better measure of the overall error budget in each individual measurement.

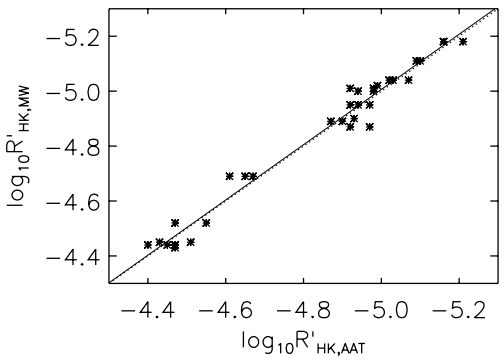

Figure 3. Derived $\log R'_{HK}$ chromospheric activities for the calibration stars on the AAPS target list. The solid line is a least-squares fit with a slope of 1.006 and a zero-point offset of 0.023. This result highlights the close relationship between the AAT and MW measurements. The dotted line is a direct 1:1 relationship.

4 DISCUSSION

Table 2 includes new and updated $\log R'_{\rm HK}$ activities for 21 planetary systems from the AAPS. It must be noted that many more stars on this list probably have planetary systems that are still awaiting discovery or are below the detectability threshold of current radial-velocity surveys. We also include the observations from Tinney et al. (2002) using our new MW activity calibration. Most of these planetary hosts had previously derived $\log R'_{\rm HK}$ values (e.g. Henry et al. 1996; Wright et al. 2004; Saffe, Gómez & Chavero 2005). Gray et al. (2006) have recently completed the analysis of stars in the Southern hemisphere for the NStars Project, and the values given here are mostly in agreement with this work. However, the agreement with this work is not as tight as with Wright et al. (2004), most likely due to the different setups employed in this study as the Gray et al. approach used 4-Å bandpasses, as opposed to the 1.09 Å used in this work and the MW Project. Indeed, when we increase the widths of our bandpasses here, non-linear calibrations are needed on to the MW system.

Knowledge of the level of activity-induced jitter in any radial-velocity measurement is essential to quantify the errors on a detected planetary fit. Jitter can vary on a time-scale of days due to a number of different factors, such as magnetic flux tube evolution, sub-photospheric convection, stellar oscillations and surface rotation of spots (Marcy et al. 2005) and can thus have a significant bearing on radial-velocity measurements. Therefore, determining the jitter level of independent measurements allows one to generate a more precise velocity point and hence a more precise overall Keplerian fit.

The 21 planetary systems in this work have $\log R'_{\rm HK}$ values ranging from -5.35 (HD 27442) to -4.43 (HD 22049). HD 22049 (aka. Eps Eri) already had measurements taken at MW and they agree with our derived mean value of -4.43, confirming the high activity of the host star. Saar, Butler & Marcy (1998), Santos et al. (2000) and Wright (2005) have carried out studies probing the relationship between stellar activity and radial-velocity jitter ($\sigma'_{\rm rv}$). Wright provides an empirical estimate of jitter, culminating in a jitter metric ($\sigma'_{\rm rv}$), which is a function of stellar evolution. [For a full detailed description of the analysis, see equations 1–7 of Wright (2005)]. Applying this methodology, and using *Hipparcos* $B-V$, $M_{\rm V}$ and a $T_{\rm EFF}$ from Valenti & Fischer (2005), we find the jitter level for the most active planet-host star in our catalogue (HD 22049) to be $\sim$5.7 m s^{-1} with 20th and 80th percentiles of 4.6 and 9.5 m s^{-1}, respectively (see Wright appendix for an explanation of percentiles). This low level of jitter for such an active star arises because the star is spectral type K. Jitter falls off at later spectral types allowing lower radial-velocity trends to be found around active K stars than F stars. The radial-velocity amplitude (K) for HD 22049 is 19 ± 1.7 m s^{-1} (Hatzes et al. 2000). This level of velocity is significantly above our derived jitter. We therefore conclude that activity is not the source of the radial-velocity signature for HD 22049.

Two other planet-host stars are shown to be quite active, both have $\log R'_{\rm HK,AAT}$ values larger than Eps Eri. The first of these is HD 13445 and it has a $\log R'_{\rm HK,AAT}$ of -4.64. As this star is a K-dwarf, the level of jitter it exhibits is not extremely high but it should be in the range 6–13 m s^{-1}. The planetary fit to this star has an amplitude of 380 ± 1 m s^{-1} with a period of 15.78 d, and from this a minimum mass of $\sim 4\,M_{\rm J}$ was derived for the planet (Queloz et al. 2000). It is clear the jitter for this star is significantly lower than the observed radial-velocity measurements. The second of the two stars is HD 17051 (ι Hor) and it has a $\log R'_{\rm HK,AAT}$ value of -4.59. Kürster et al. (2000) announced the detection of a planet with a minimum mass of $2.26 M_{\rm J}$ and a period of 320.1 ± 2.1 d. The amplitude of the planetary fit is 67 m s^{-1} with a rms scatter of 27 m s^{-1}. The internal errors were estimated to be 17 m s^{-1} and they speculated the difference was activity induced, with a jitter of 20 m s^{-1} making up this difference. Butler et al. (2001) obtained a rms of 10.4 m s^{-1} for this star using measurements made at the AAT and Saar et al. (1998) find a jitter of 10 m s^{-1}, consistent with the AAT scatter. A further 10 measurements have been taken by Bulter et al. since 2001 over a period of 4 yr and the current best-fitting single-planet Keplerian has a rms of 20 m s^{-1}, consistent with the results from Kürster et al. (2000). We find a jitter range of 9–19 m s^{-1}, which agrees well with observations, and the higher end of this range can go a long way towards explaining the high level of scatter observed by Kürster et al. (2000) and Butler et al. (private communication).

17 out of the other 18 remaining planet-hosts objects are relatively inactive. These are HD 142, HD 2039, HD 20782, HD 23079, HD 27442, HD 30177, HD 70642, HD 73526, HD 76700, HD 102117, HD 134987, HD 142415, HD 154857, HD 169830, HD 179949, HD 216435 and HD 216437. We find that the derived jitter value cannot explain the observed stellar radial-velocity signal confirming the planetary hypothesis. However, the remaining star (HD 10647) is spectral type F and we find the radial-velocity jitter is likely to be similar to the reported planetary signal. At the 2003 conference 'Extrasolar Planets: Today and Tomorrow', Mayor announced a best-fitting Keplerian to the data with a K of 18 ± 1 m s^{-1}, giving rise to a planet with a period of 1040 d (2.85 yr) and a $M \sin i$ of $\sim 0.91\,M_{\rm J}$ for HD 10647. We find the $\log R'_{\rm HK,AAT}$ index to be -4.70. This relates to a jitter of $\sim$11–23 m s^{-1} at the 1σ level. This level of jitter is similar to the derived planetary signature. The star also exhibits a strong infrared (IR) excess (Decin et al. 2000) which may be indicative of the presence of a disc. This also agrees well with the active nature of the star as this indicates the star is young. Mayor acknowledged the jitter phenomenon, and by the use of a bisector analysis, they found no evidence for any periodic line profile variability. Jones et al. (2004) find only weak evidence for a planetary companion in the AAPS data set for this object. However, four additional measurements have been taken at the AAT for this star over a period of 2 yr. The current best-fitting Keplerian has a period of 2.73 yr with an amplitude of 17.9 m s^{-1}. The rms to the fit is 8.9 m s^{-1} (Butler et al. 2006). This signature is in agreement with the signal announced by Mayor; however with a false alarm probability of 0.25, more data points will be needed to obtain robust planetary parameters.

4.1 $\log R'_{\rm HK}$ distribution

Fig. 4 shows the distribution of stellar activity for 225 stars on the AAPS target list. The selection criteria for the list itself target more evolved stars, and as such the inactive peak was expected. We see the indication of a possible binomial distribution in activity with peaks centred at -4.95 and -4.45. This result has been found before in both the Northern and Southern hemispheres (e.g. Vaughan & Preston 1980; Henry et al. 1996).

There are a number of highly active ($\log R'_{\rm HK} > -4.5$) stars on this list. For the assessment of highly active stars, we use the Santos et al. (2000) jitter relation [see equations 2–4 from Santos et al. (2000)], as the Wright model is out of range for some of our active stars. The vertical solid line in Fig. 4 represents the lower boundary of these active stars. There are 19 stars in this region. Since the $R'_{\rm HK}$–σ'(Vr) relation decreases with spectral type, the jitter values of half of these are closer to the lower end of this range, as nine of these stars are K-dwarfs. However, all are expected to have jitter values in excess

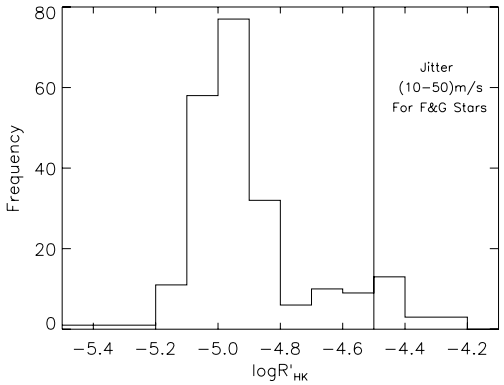

Figure 4. A histogram of the $\log R'_{\rm HK}$ activity index distribution for the stars on the AAPS target list. It is clear that the majority of the stars observed by the AAPS are inactive, with the peak residing at values below −4.90. The solid vertical line bounds the region inhabited by very active stars. The lower limit radial-velocity jitter range is shown for F and G stars in this region.

of ∼7 m s^{-1}; therefore the low-amplitude radial-velocity signatures of companions must be treated with care. Also, two of the active set are M-dwarfs, and with $B - V$ colours >1.5 they are outside the model limits for jitter determination. Wright (2005) shows that M-type stars statistically exhibit higher jitter levels than F-, G- and K-type stars. Therefore, we expect these two active M stars to exhibit high levels of jitter.

Analysis of the remaining F- and G-type stars, HD 1835, HD 11131, HD 13246, HD 19632, HD 88201, HD 90712, HD 129060 and HD 152391, shows that these are likely to have jitter values around ∼10–30 m s^{-1}. HD 1835 and HD 11131 were used as calibrators, and both the MW and CTIO studies have found these to be highly active. This level of jitter has already proven sufficient to mimic a planetary companion (e.g. Queloz et al. 2001; Henry et al. 2002). It must be noted that the $\log R'_{\rm HK} > -4.5$ is a somewhat arbitrary cut-off. An F-type star, such as HD 16673, with a $\log R'_{\rm HK}$ value of −4.64, still provides a jitter range of around: $\sigma \sim 11$–24 ms^{-1}. Therefore, it is necessary to take great care when dealing with radial-velocity amplitudes for all F-type stars > −4.70. Indeed, the two active F-type stars (HD 13246 and HD 129060) exhibit extremely high levels of jitter. Having $\log R'_{\rm HK}$ values of −4.38 and −4.41, respectively, they exhibit jitter of around ∼17–40 m s^{-1}. This level of jitter puts serious limitations on the potential for planet discoveries around these stars. The AAPS baseline is 8 yr and even giant planets with orbital periods longer than this do not generate large radial-velocity amplitudes. For example, Jupiter, with a semi-major axis of 5.2 au, induces a radial-velocity motion of ∼12 m s^{-1} on the Sun over a 12-yr period. The jitter level exhibited by both these stars could serve to mask the planetary signature of an orbiting Jupiter even once the baseline is sufficient to detect them.

Due to the variable nature of stellar activity, in particular when dealing with active stars, it is important to obtain multi-epoch activity indices. This will allow planet searches to state categorically that the jitter-level is significantly lower than any companion's periodic radial-velocity signature. It is even more essential in the Southern hemisphere, where no such program yet exists. We have obtained more than one measurement for a small number of our stars, but with a maximum of three observations, we are still limited by a lack of data. At MW, a number of measurements are obtained of the same object over an observing season. The difference in $\log R'_{\rm HK}$-index over one season can change at the level of $\sim \pm 0.2$ [see Duncan et al. 1991, table 1 column 5). This variation was recorded using a single well-defined setup (e.g. HD 16673: 202 measurements: $-4.66 \leqslant \log R'_{\rm HK} \leqslant -4.82$). Another example would be our own parent star. The $\log R'_{\rm HK}$-index of the Sun varies from its typical value of ~ -5.10 to −4.96 during the Solar minimum (Wright et al. 2004). This level of discrepancy highlights the difficulty when attempting to calibrate between systems and when trying to fully quantify activity. This is why gaining multiple measurements using a well-defined standard setup is essential.

Time series analysis also allows other avenues of study to be undertaken. Stellar ages and rotation periods can be empirically estimated using $\log R'_{\rm HK}$ relationships. For instance, the age–chromospheric activity relation of Soderblom, Duncan & Johnson (1991), most recently updated to its current form by Baliunas et al. (1995) and taken from Wright (2005), is given by

$$\log[t(\mathrm{yr})] = -0.0522R_5^3 + 0.4085R_5^2 - 1.334R_5 + 10.725 \qquad (3)$$

here $R_5 = 10^5\ R'_{\rm HK}$ and $R'_{\rm HK}$ represents the activity level for a solar-type star averaged over many stellar activity cycles. The more observations one obtains, the closer one gets to the actual age derived from this relationship. This is because taking multiple measurements allows a better determination of the mean activity index for main-sequence stars. Using the Sun's variability range from above (~ -5.10 to −4.96) causes measurements of the solar age to differ by several Gyr (e.g. 7.92–4.93 Gyr). Variability knowledge is essential to obtain reliable age and rotation estimates of stars.

ACKNOWLEDGMENT

We acknowledge the comments made by the anonymous referee.

REFERENCES

Baliunas S. L., Donahue R. A., Soon W., Gilliland R., Soderblom D. R., 1995, BAAS, 27, 839
Butler R. P., Tinney C. G., Marcy G. W., Jones H. R. A., Penny A. J., Apps K., 2001, ApJ, 555, 410
Butler R. P. et al., 2006, ApJ, 646, 505
Decin G., Dominik C., Malfait K., Mayor M., Waelkens C., 2000, A&A, 357, 533
Duncan D. K. et al., 1991, ApJS, 76, 383
Gray R. O., Corbally C. J., Garrison R. F., McFadden M. T., Bubar E. J., McGahee C. E., O'Donoghue A. A., Knox E. R., 2006, AJ, 132, 161
Hatzes A. P. et al., 2000, ApJ, 544, L145
Henry G. W., Donahue R. A., Baliunas S. L., 2002, ApJ, 577, L111
Henry T. J., Soderblom D. R., Donahue R. A., Baliunas S. L., 1996, AJ, 111, 439
Jones H. R. A., Paul Butler R., Marcy G. W., Tinney C. G., Penny A. J., McCarthy C., Carter B. D., 2002, MNRAS, 337, 1170
Jones H. R. A., Butler R. P., Tinney C. G., Marcy G. W., McCarthy C., Penny A. J., Carter B. D., 2004, in Beaulieu J.-P., des Etangs A. L., Terquem C., eds, ASP Conf. Ser. Vol. 321, Extrasolar Planets: Today and Tomorrow. Astron. Soc. Pac., San Francisco, p. 298
Kürster M., Endl M., Els S., Hatzes A. P., Cochran W. D., Döbereiner S., Dennerl K., 2000, A&A, 353, L33
Marcy G. W., Butler R. P., Vogt S. S., Fischer D. A., Henry G. W., Laughlin G., Wright J. T., Johnson J. A., 2005, ApJ, 619, 570
Mills D., Webb J., Clayton M., 1996, Starlink, 152, 1
Noyes R. W., Hartmann L. W., Baliunas S. L., Duncan D. K., Vaughan A. H., 1984, ApJ, 279, 763
Paulson D. B., Cochran W. D., Hatzes A. P., 2004, AJ, 127, 3579
Queloz D. et al., 2000, A&A, 354, 99
Queloz D., Henry G. W., Sivan J. P., Baliunas S. L., 2001, A&A, 379, 279
Saar S. H., Donahue R. A., 1997, ApJ, 485, 319
Saar S. H., Butler R. P., Marcy G. W., 1998, ApJ, 498, L153
Saffe C., Gómez M., Chavero C., 2005, A&A, 443, 609

Santos N. C., Mayor M., Naef D., Pepe F., Queloz D., Udry S., Blecha A., 2000, A&A, 361, 265
Santos N. C. et al., 2002, A&A, 392, 215
Soderblom D. R., Duncan D. K., Johnson D. R. H., 1991, ApJ, 375, 722
Strassmeier K., Washuettl A., Granzer T., Scheck M., Weber M., 2000, A&AS, 142, 275
Tinney C. G., Butler R. P., Marcy G. W., Jones H. R. A., Penny A. J., Vogt S. S., Apps K., Henry G. W., 2001, ApJ, 551, 507
Tinney C. G., McCarthy C., Jones H. R. A., Butler R. P., Carter B. D., Marcy G. W., Penny A. J., 2002, MNRAS, 332, 759
Turnshek D. A., Bohlin R. C., Williamson R. L., Lupie O. L., Koornneef J., Morgan D. H., 1990, AJ, 99, 1243
Valenti J. A., Fischer D. A., 2005, ApJS, 159, 141
Vaughan A. H., Preston G. W., 1980, PASP, 92, 385
Wright J. T., 2005, PASP, 117, 657
Wright J. T., Marcy G. W., Butler R. P., Vogt S. S., 2004, ApJS, 152, 261

This paper has been typeset from a TEX/LATEX file prepared by the author.